Stability analysis for two coupled synchronous generators

Elad Venezian * **George Weiss** **

* *School of EE, Tel Aviv University Ramat Aviv 69978, Israel (e-mail: eladv@gmail.com)*
** *School of EE, Tel Aviv University Ramat Aviv 69978, Israel (e-mail: gweiss@eng.tau.ac.il)*

Abstract: We investigate the stability of a microgrid composed of two identical synchronous generators, inductive lines and resistive loads, without using any model reduction for "fast" variables. We derive sufficient conditions for local exponential stability, with a region of attraction that includes any initial state such that the states of the generators are sufficiently close to each other. This implies that if by some control technique we can bring the angular velocities close enough, regardless how far the system is from the equilibrium state, then the generators will synchronize.

Keywords: synchronous generator, microgrid, synchronization, local stability, invariant manifold, region of attraction.

1. INTRODUCTION

The grid is an enormously complex nonlinear and randomly varying system for which rigorous stability analysis is impossible. Many techniques and models that have been developed to assess the stability of a power grid, using simplifying assumptions and reduced models, see for instance Kundur (1994), Grainger et al. (1994), Sauer et al. (1997), Galaz et al. (2003), Dörfler at al. (2012).

In recent years, due to the increasing penetration of renewable energy resources, which connect to the grid via power converters and produce an intermittent power output, it is not clear whether the traditional models and methods for controlling the power grid will succeed to control it. Therefore, there is an increasing interest in the fundamental mathematical models and stability analysis for the grid, see for instance Dörfler at al. (2012), Simpson-Porco et al. (2013), Caliskan et al. (2014), Natarajan et al. (2014), Natarajan et al. (2015), Monshizadeh et al. (2016).

An important concept that facilitate the integration of the renewable energy resources into the electricity grid is the microgrid concept Green et al. (2007); Schiffer et al. (2016). A microgrid can work as an independent isolated network (islanded mode), or alternatively in grid connected mode it behaves as a single controllable generator or load from the viewpoint of the remaining electrical system. In islanded mode, the frequency, voltage and power sharing are actively controlled within the microgrid. Controlling the frequency and voltage and balance the active/reactive load demand, is one of the main challenges of the microgrid system Shafiee et al. (2016); Zhong (2013).

The *synchronous generator* (SG) is the main power source of the electricity grid. The mathematical model of a SG (see the earlier references and in addition Walker (1981), Fitzgerald et al. (2003), Mandel et al. (2015), etc.) is complex and difficult to use as a component when we model a large network. Stability analysis is usually done either by simulation, or analytically on simplified models, in which the SGs are connected in a simple network and each SG is represented by reduced order equations, see for instance Dörfler at al. (2012) and Simpson-Porco et al. (2013). The reduced model of a SG is often obtained by treating the stator currents as fast variables, thus eliminating them from the state variables via the singular perturbation approach (see, for instance, Khalil (2002)) and keeping only the rotor angle, the rotor angular velocity and the rotor field as relevant state variables, see for instance Kundur (1994) and Sauer et al. (1997).

It is desirable to know if for a given grid which contains SGs and a loads, the SGs tend to synchronize (for initial states in a reasonably large region) and if yes, if the grid frequency and power flows remains stable.

Here we study a microgrid composed of a two identical SGs connected to a resistive load, as shown in Figure 1. These generators are driven by identical prime movers, that have frequency droop control. Our main result is that if the difference between the initial states of the SGs is sufficiently small, then the state of the entire system converges at an exponential rate to a unique stable equilibrium point in the state space $\mathcal{X}$, a 7-dimensional manifold. In $\mathcal{X}$, the angle difference δ between the generators is counted modulo 2π. In some arguments we use $\mathbb{R}^7$ as a state space, and then δ can take any real value.

We illustrate our results by simulations. In particular, we show an example of two SGs where the region of attraction of the stable equilibrium point contains the submanifold where the generators have equal states (as it always does), but it does not contain all $\mathcal{X}$.

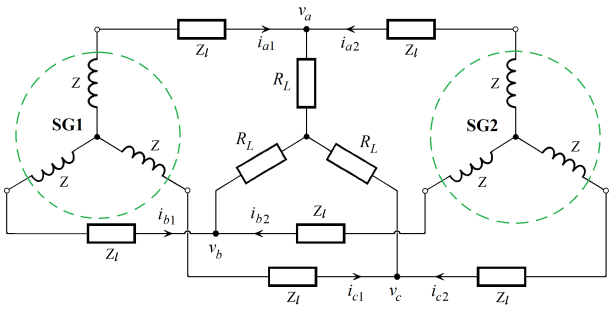

Fig. 1. The two identical coupled SGs (TICSG) model, showing the stator windings, the line impedances Z_l and the load resistors R_L, but not showing the rotor windings or the prime movers.

2. MODELING A SINGLE SG

We recall the equations for a SG connected to an exernal voltage and having a constant field (or rotor) current i_f, following the notation in Zhong et al. (2011), see also Natarajan et al. (2014, 2015), Venezian et al. (2016).

The rotor of a SG is a coil on a magnetic core that spins inside a circular cavity in the stator, having the angle θ with respect to a reference angle. We consider that there is no neutral connection and no damper windings. The stator windings can be regarded as connected coils with self inductance L, mutual inductance $-M$, and resistance R_s (the parameters L_f, R_f, L, M, R_s are positive). We assume no magnetic saturation effects in the iron core and no Eddy currents. The stator terminals are labeled with the letters a, b, c and the vector of voltages on the stator terminals is denoted by $v = [v_a \ v_b \ v_c]^\top$.

The mutual inductance between the rotor coil and each of the stator coils is a sinusoidal function of θ, with amplitude $M_f > 0$. In order to represent the voltages and currents in a more convenient way, we apply the Park transformation with respect to the rotor angle, obtaining the voltages v_d, v_q, v_0 and the currents i_d, i_q, i_0. We denote

$$\omega = \dot\theta, \qquad m = \sqrt{\frac{3}{2}} M_f.$$

As shown in the sources cited at the beginning of this section, we obtain the following model for a SG:

$$\frac{\mathrm{d}}{\mathrm{d}t}\begin{bmatrix} L_s i_d \\ L_s i_q \\ J\omega \end{bmatrix} = \begin{bmatrix} -R_s & \omega L_s & 0 \\ -\omega L_s & -R_s & -m i_f \\ 0 & m i_f & -D_p \end{bmatrix} \begin{bmatrix} i_d \\ i_q \\ \omega \end{bmatrix} + \begin{bmatrix} -v_d \\ -v_q \\ T_m \end{bmatrix}, \quad (1)$$

where J is the moment of inertia of the rotor, $T_m - D_p\omega$ is is the torque coming from the prime mover, D_p is a the frequency droop coefficient employed in the prime movers connected to the generators. If any viscous friction is present, it can be absorbed into the term $D_p\omega$. The parameters J, T_m, D_p are positive. The feedback term $D_p\omega$ is used to control the frequency of the grid, see Kundur (1994), Simpson-Porco et al. (2013), Caliskan et al. (2014), Zhong et al. (2011).

3. TICSG MODELING

In this section we develop the TICSG model that represent two identical SGs connected to a common resistive load, as

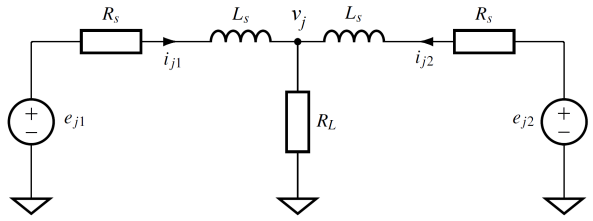

Fig. 2. The TICSG model - equivalent circuit for one phase, $j \in \{a, b, c\}$.

shown in Figure 1, assuming constant field currents. The model of each SG is as in Section 2.

We denote the SG rotor angles by θ_1 and θ_2 and $\omega_1 = \dot\theta_1$, $\omega_2 = \dot\theta_2$. We assume that identical prime movers act on the generators, producing the torques $T_m - D_p\omega_i$, $i \in \{1, 2\}$. By symmetry, we assume that the voltages at the (non-connected) midpoints of the generators and the load are zero. We denoted the phase voltages on the load by $v = [v_a \ v_b \ v_c]^\top$, the currents of the first generator by $i_1 = [i_{a1} \ i_{b1} \ i_{c1}]^\top$ and similarly for the currents of the second generator.

In Figure 1 we have indicated by Z the equivalent impedance of each SG stator, $Z = sL_s + R_s$. The line that connects the SG to the load has its impedance Z_l that can be modeled as a resistance and an inductance in series, but these values can simply be added to the parameters R_s and L_s of the SG. After this simplification, each phase of the circuit from Figure 1 is as in Figure 2.

In order to use the model (1) for each SG, we apply the Park transformation (defined in the previous section) to the load voltages, $[v_{d1} \ v_{q1} \ v_{01}]^\top = U(\theta_1)\,[v_a \ v_b \ v_c]^\top$, and to the currents $[i_{d1} \ i_{q1} \ i_{01}]^\top = U(\theta_1)\,[i_{a1} \ i_{b1} \ i_{c1}]^\top$, and similarly for i_2 and θ_2. From $v = R_L(i_1 + i_2)$ we get, after applying the Park transformation with respect to θ_1,

$$\begin{bmatrix} v_{d1} \\ v_{q1} \\ v_{01} \end{bmatrix} = R_L \begin{bmatrix} i_{d1} \\ i_{q1} \\ i_{01} \end{bmatrix} + R_L U(\theta_1) \begin{bmatrix} i_{a2} \\ i_{b2} \\ i_{c2} \end{bmatrix}.$$

Here we express the currents of the second SG by using the inverse Park transformation:

$$\begin{bmatrix} v_{d1} \\ v_{q1} \\ v_{01} \end{bmatrix} = R_L \begin{bmatrix} i_{d1} \\ i_{q1} \\ i_{01} \end{bmatrix} + R_L U(\theta_1) U(\theta_2)^{-1} \begin{bmatrix} i_{d2} \\ i_{q2} \\ i_{02} \end{bmatrix}. \quad (2)$$

We denote $\delta = \theta_2 - \theta_1$.

A simple computation shows that

$$U(\theta_1)U(\theta_2)^{-1} = \begin{bmatrix} \cos(\delta) & -\sin(\delta) & 0 \\ \sin(\delta) & \cos(\delta) & 0 \\ 0 & 0 & 1 \end{bmatrix}. \quad (3)$$

Since the SGs don't have a neutral connection, from Kirchhoff's laws we obtain that $i_{01} = i_{02} = 0$. Substituting this into (2) and (3) shows that $v_{01} = 0$.

Substituting (3) and (2) into (1) gives:

$$\Lambda \dot z_1 = \mathcal{A}(\omega_1) z_1 + T_m e_3 - \mathcal{B}(\delta) z_2,$$

where we have denoted

$$z_i = [i_{di} \ i_{qi} \ \omega_i]^\top, \quad i \in \{1, 2\}, \quad (4)$$

$$\Lambda = \begin{bmatrix} L_s & 0 & 0 \\ 0 & L_s & 0 \\ 0 & 0 & J \end{bmatrix},$$

$$\mathcal{A}(\omega) = \begin{bmatrix} -R_{tot} & \omega L_s & 0 \\ -\omega L_s & -R_{tot} & -mi_f \\ 0 & mi_f & -D_p \end{bmatrix},$$

$$\mathcal{B}(\delta) = \begin{bmatrix} R_L\cos(\delta) & -R_L\sin(\delta) & 0 \\ R_L\sin(\delta) & R_L\cos(\delta) & 0 \\ 0 & 0 & 0 \end{bmatrix},$$

$$e_3 = [0\ 0\ 1]^\top, \quad R_{tot} = R_s + R_L.$$

A symmetric equation holds for the second generator:

$$\Lambda \dot{z}_2 = \mathcal{A}(\omega_2) z_2 + T_m e_3 - \mathcal{B}(-\delta) z_1 .$$

An additional ODE for δ is:

$$\dot{\delta} = \omega_2 - \omega_1 .$$

Rewriting the entire TICSG system dynamics gives:

$$\frac{\mathrm{d}}{\mathrm{d}t}\begin{bmatrix} \Lambda z_1 \\ \Lambda z_2 \\ \delta \end{bmatrix} = \left[\begin{array}{c|c|c} \mathcal{A}(\omega_1) & -\mathcal{B}(\delta) & 0 \\ -\mathcal{B}(-\delta) & \mathcal{A}(\omega_2) & 0 \\ -e_3^T & e_3^T & 0 \end{array}\right] \begin{bmatrix} z_1 \\ z_2 \\ \delta \end{bmatrix} + T_m \begin{bmatrix} e_3 \\ e_3 \\ 0 \end{bmatrix}. \quad (5)$$

Proposition 3.1. The TICSG system is forward complete, i.e. for any initial state $\left[z_1^{0\top}\ z_2^{0\top}\ \delta^0\right]^\top \in \mathbb{R}^7$, the (unique) solution of the TICSG system is defined for all $t > 0$.

Sketch of the proof. The right hand-side of the TICSG model (5) is a locally Lipschitz function on the state space $\mathbb{R}^7$. For any initial state it follows from standard well posedness results (see for instance (Khalil, 2002, Ch. 3)) that there exists a unique solution (z_1, z_2, δ) for (5) defined on a maximal time interval $[0, T_{\max})$, with $T_{\max} > 0$, possibly $T_{\max} = \infty$. For any $(z_1, z_2) \in \mathbb{R}^6$ define

$$V(z_1, z_2) = \frac{1}{2}\left[z_1^\top\ z_2^\top\right]\begin{bmatrix} \Lambda & 0 \\ 0 & \Lambda \end{bmatrix}\begin{bmatrix} z_1 \\ z_2 \end{bmatrix}. \quad (6)$$

Then, using (5), we can show that along state trajectories, $\dot{V}(t)$ is a quadratic expression in the state variables plus first order terms, and the quadratic part is negative definite. Hence, if the norm of the state vector is large enough, then $\dot{V}(t) < 0$. Therefore V (and hence i_{d1}, i_{q1}, ω_1, i_{d2}, i_{q2} and ω_2) are bounded on $[0, T_{\max})$. If $T_{\max}$ would be finite, then δ would also be bounded on $[0, T_{\max})$, which contradicts Theorem 3.3 (p. 94) in Khalil (2002). Therefore $T_{\max} = \infty$. The details of this proof will be in the journal version of this paper. □

Proposition 3.2. We work with the function V from (6). For all $\mu > 0$ sufficiently large, the set

$$\mathcal{K}^\mu = \left\{[z_1^\top\ z_2^\top\ \delta]^\top \in \mathbb{R}^7 \mid V(z_1, z_2) \le \mu\right\}$$

is invariant under the flow of the TICSG system (5).

Proof. We know from the proof of Proposition 3.1 that $\dot{V}$ can be expressed as a quadratic expression flus first order terms, and the quadratic expression is negative. It is easy to see that the set K_+ of those $(z_1, z_2) \in \mathbb{R}^6$ where $\dot{V} \ge 0$ is compact. Let

$$\mu_0 = \max\{V(z_1, z_2) \mid (z_1, z_2) \in K_+\}.$$

Then for any $\mu > \mu_0$ we have that $V(z_1, z_2) = \mu$ implies $\dot{V} < 0$. Hence, the trajectories of the TICSG system cannot exit the set $\mathcal{K}^\mu$, so that this set is invariant. □

Sometimes we find it more convenient to consider the angle δ modulo 2π, so that the seventh coordinate of the state is no longer in $\mathbb{R}$, but instead in the unit circle $\mathcal{C}$. This new state space $\mathcal{X}$ is a 7 dimensional manifold, with a natural mapping ϕ from $\mathbb{R}^7$ to $\mathcal{X}$ (which leaves the first 6 coordinates unchanged). If we define (for $\mu > \mu_0$)

$$\mathcal{K}^\mu_{\mathcal{X}} = \phi\mathcal{K}^\mu,$$

then $\mathcal{K}^\mu_{\mathcal{X}}$ is a compact invariant set for the TICSG system in the state space $\mathcal{X}$.

4. THE EQUILIBRIUM POINTS OF THE TICSG MODEL

In this section we study the equilibrium points of the TICSG system (5). We introduce the *synchronization subspace* of the state space $\mathbb{R}^7$ by

$$\mathcal{E} = \left\{[z_1\ z_2\ \delta]^\top \in \mathbb{R}^7 \mid z_1 = z_2,\ \delta = 0\right\}. \quad (7)$$

Clearly this is a 3-dimensional vector subspace. Similarly, we introduce the *anti-synchronization space*

$$\mathcal{E}' = \left\{[z_1\ z_2\ \delta]^\top \mid z_1 = z_2,\ \delta = \pi\right\}, \quad (8)$$

which is an affine space (shifted vector subspace). Recall from Section 3 that sometimes we prefer to consider the angle δ modulo 2π, so that the state space $\mathcal{X}$ is a 7 dimensional manifold, with a natural mapping ϕ from $\mathbb{R}^7$ onto $\mathcal{X}$. The images of $\mathcal{E}$ and $\mathcal{E}'$ via ϕ are 3 dimensional submanifolds of $\mathcal{X}$ that we denote by $\mathcal{E}_{\mathcal{X}}$ and $\mathcal{E}'_{\mathcal{X}}$, respectively. We call $\mathcal{E}_{\mathcal{X}}$ the *symchronization manifold.*

Proposition 4.1. Any equilibrium point for the TICSG system in $\mathcal{X}$ is either in $\mathcal{E}_{\mathcal{X}}$ or in $\mathcal{E}'_{\mathcal{X}}$.

The proof will be in the journal version of this paper.

Proposition 4.2. The TICSG system has at least one equilibrium point on synchronization subspace $\mathcal{E}$ from (7).

Sketch of the proof. We have to show that there exists $z^e = [i_d^e\ i_q^e\ \omega^e]^\top \in \mathbb{R}^3$ such that the point $[z^{e\top}\ z^{e\top}\ 0]^\top \in \mathcal{E}$ is an equilibrium point of the TICSG system. It is easy to see that this happens if and only if

$$\begin{bmatrix} -R_s - 2R_L & \omega^e L_s & 0 \\ -\omega^e L_s & -R_s - 2R_L & -mi_f \\ 0 & mi_f & -D_p \end{bmatrix}\begin{bmatrix} i_d^e \\ i_q^e \\ \omega^e \end{bmatrix} = \begin{bmatrix} 0 \\ 0 \\ -T_m \end{bmatrix}. \quad (9)$$

From (9) we derive by some computations a scalar equation to determine the equilibrium velocity ω^e: denoting $R_T = R_L + R_{tot}$, we get the cubic equation

$$D_p L_s^2 \omega^{e3} - T_m L_s^2 \omega^{e2} + \left(D_p R_T^2 + m^2 i_f^2 R_T\right)\omega^e - T_m R_T^2 = 0.$$

Let us denote the polynomial of order 3 appearing above by p. Clearly

$$p(0) = -T_m R_T^2 < 0.$$

On the other hand, we note that

$$p\left(\frac{T_m}{D_p}\right) = m^2 i_f^2 R_T \frac{T_m}{D_p} > 0.$$

Hence, p has at least one zero in the interval $\left(0, \frac{T_m}{D_p}\right)$. This shows that the TICSG system has at least one equilibrium point located on the synchronization subspace (7). □

Note that $\mathcal{E}'_{\mathcal{X}}$ may also contain equilibrium points.

5. THE SYNCHRONIZED SYSTEM

If the state of the TICSG system (5) is in the synchronization subspace $\mathcal{E}$ from (7), it means that the two generators

are perfectly synchronized. We show that $\mathcal{E}$ is invariant under the flow of the system (5) and the restriction of this flow to $\mathcal{E}$ is globally asymptotically stable.

The TICSG system has the following structure:

$$\tilde{\Lambda}\frac{\mathrm{d}}{\mathrm{d}t}\left[z_1\ z_2\ \delta\right]^\top = f\left(\left[z_1\ z_2\ \delta\right]^\top\right),$$

where $\tilde{\Lambda} = \mathrm{diag}\,(\Lambda, \Lambda, 1)$. In order to show synchronization, it is convenient to introduce new state variables $e \in \mathbb{R}^4$ and $x \in \mathbb{R}^3$ by

$$e = \begin{bmatrix} z_2 - z_1 \\ \delta \end{bmatrix} = \left[e_d\ e_q\ e_\omega\ \delta\right]^\top$$

and

$$x = z_1 + z_2 = \left[x_d\ x_q\ x_\omega\right]^\top.$$

Then the TICSG model (5) can be rewritten as

$$\dot{e} = F(e,x), \qquad \dot{x} = G(e,x), \tag{10}$$

for some smooth functions F and G. From (5),

$$\begin{aligned}\Lambda(\dot{z}_2 - \dot{z}_1) = {} & \mathcal{A}(\omega_2)z_2 + T_m e_3 - \mathcal{B}(-\delta)z_1 \\ & - \left(\mathcal{A}(\omega_1)z_1 + T_m e_3 - \mathcal{B}(\delta)z_2\right).\end{aligned}$$

The detailed form of the equation $\dot{e} = F(e,x)$ is

$$\begin{bmatrix}\Lambda & 0\\ 0 & 1\end{bmatrix}\frac{\mathrm{d}}{\mathrm{d}t}\begin{bmatrix} e_d \\ e_q \\ e_\omega \\ \delta\end{bmatrix} =$$

$$\begin{bmatrix} -R_{tot}(i_{d2} - i_{d1}) + L_s(\omega_2 i_{q2} - \omega_1 i_{q1}) \\ -L_s(\omega_2 i_{d2} - \omega_1 i_{d1}) - R_{tot}(i_{q2} - i_{q1}) - m i_f(\omega_2 - \omega_1) \\ m i_f(i_{q2} - i_{q1}) - D_p(\omega_2 - \omega_1) \\ -(\omega_2 - \omega_1)\end{bmatrix}$$

$$+\begin{bmatrix} R_L\cos(\delta)(i_{d2} - i_{d1}) - R_L\sin(\delta)(i_{q2} + i_{q1}) \\ R_L\cos(\delta)(i_{q2} - i_{q1}) + R_L\sin(\delta)(i_{d2} + i_{d1}) \\ 0 \\ 0\end{bmatrix}.$$

From a simple computation, the previous equation can be rewritten as

$$\dot{e} = F(e,x) = \begin{bmatrix}\Lambda & 0\\ 0 & 1\end{bmatrix}^{-1}\left[A_e\,(e,x)\,e + B_e\,(e,x)\right], \tag{11}$$

where

$$A_e\,(e,x) =$$

$$\begin{bmatrix} -R_{tot} + R_L\cos\delta & \frac{L_s}{2}x_\omega & \frac{L_s}{2}x_q & 0 \\ -\frac{L_s}{2}x_\omega & -R_{tot} + R_L\cos\delta & -\frac{L_s}{2}x_d - m i_f & 0 \\ 0 & m i_f & -D_p & 0 \\ 0 & 0 & 1 & 0\end{bmatrix}$$

and

$$B_e\,(e,x) = \begin{bmatrix} -R_L\sin(\delta)x_q \\ R_L\sin(\delta)x_d \\ 0 \\ 0\end{bmatrix}.$$

Note that the synchronization subspace $\mathcal{E}$ from (7), in the new coordinates, becomes $\mathcal{E} = \left\{\begin{bmatrix}x\\ e\end{bmatrix} \in \mathbb{R}^7 |\ e = 0\right\}$. We note that $F(0,x) = 0$, which shows that $\mathcal{E}$ is invariant.

For the x dynamics we have

$$\begin{aligned}\Lambda\dot{x} = {} & \mathcal{A}(\omega_1)z_1 + T_m e_3 - \mathcal{B}(\delta)z_2 \\ & + \mathcal{A}(\omega_2)z_2 + T_m e_3 - \mathcal{B}(-\delta)z_1,\end{aligned}$$

$$\Lambda\frac{\mathrm{d}}{\mathrm{d}t}\begin{bmatrix} x_d \\ x_q \\ x_\omega\end{bmatrix} =$$

$$\begin{bmatrix} -R_{tot}(i_{d1} + i_{d2}) + L_s(\omega_1 i_{q1} + \omega_2 i_{q2}) \\ -L_s(\omega_1 i_{d1} + \omega_2 i_{d2}) - R_{tot}(i_{q1} + i_{q2}) - m i_f(\omega_1 + \omega_2) \\ m i_f(i_{q1} + i_{q2}) - D_p(\omega_1 + \omega_2) + 2T_m\end{bmatrix}$$

$$+\begin{bmatrix} -R_L\cos(\delta)(i_{d1} + i_{d2}) - R_L\sin(\delta)(i_{q1} - i_{q2}) \\ -R_L\cos(\delta)(i_{q1} + i_{q2}) + R_L\sin(\delta)(i_{d1} - i_{d2}) \\ 0\end{bmatrix}.$$

It is easy to check that this can be rewritten as:

$$\dot{x} = G\,(e,x) = \Lambda^{-1}\left(A_x\,(e,x)\,x + B_x\,(e,x)\right), \tag{12}$$

where

$$A_x\,(e,x) = \begin{bmatrix} -R_{tot} - R_L\cos(\delta) & L_s x_\omega/2 & 0 \\ -L_s x_\omega/2 & -R_{tot} - R_L\cos(\delta) & -m i_f \\ 0 & m i_f & -D_p\end{bmatrix}$$

$$B_x\,(e,x) = \begin{bmatrix} L_s e_\omega e_q/2 - R_L\sin(\delta)e_q \\ -L_s e_\omega e_d/2 - R_L\sin(\delta)e_d \\ 2T_m\end{bmatrix}.$$

Proposition 5.1. The system $\dot{x} = G(0,x)$, with state space $\mathbb{R}^3$, is globally exponentially stable if

$$16 R_T D_p > L_s^2\left(\left(x_q^e\right)^2 + \left(x_d^e\right)^2\right). \tag{13}$$

Sketch of the proof. We denote the state variables of this system by $x = \left[x_d\ x_q\ x_\omega\right]^\top$. We denote $\tilde{G}(x) = G(0,x)$. Then

$$\dot{x} = \tilde{G}(x) = \Lambda^{-1}A\,(x_\omega)\,x + \Lambda^{-1}B,$$

where we denote

$$A\,(x_\omega) = A_x\,(0,x) = \begin{bmatrix} -R_T & \frac{L_s}{2}x_\omega & 0 \\ -\frac{L_s}{2}x_\omega & -R_T & -m i_f \\ 0 & m i_f & -D_p\end{bmatrix}$$

and

$$B = B_x\,(0,x) = \begin{bmatrix} 0 \\ 0 \\ 2T_m\end{bmatrix}.$$

Because the TICSG system has at least one equilibrium point in $\mathcal{E}$ (see Proposition 4.2), using the new coordinates there exists at least one $x^e = \left[x_d^e\ x_q^e\ x_\omega^e\right]^\top \in \mathbb{R}^3$ such that $\tilde{G}(x^e) = 0$, in other words,

$$A(x_\omega^e)x^e + B = 0. \tag{14}$$

In order to shift the equilibrium point into the origin, we introduce the new coordinates

$$\hat{x} := x - x^e.$$

A natural Lyapunov function candidate for this system is

$$V(\hat{x}) := \frac{1}{2}L_s\left(\hat{x}_d^2 + \hat{x}_q^2\right) + \frac{1}{2}J\hat{\omega}^2 = \frac{1}{2}\hat{x}^T\Lambda\hat{x}.$$

It is easy to see that

$$\frac{1}{2}\min\left\{L_s, J\right\}|\hat{x}|^2 \le V(\hat{x}) \le \frac{1}{2}\max\left\{L_s, J\right\}|\hat{x}|^2,$$

$$\dot{\hat{x}} = \dot{x} = \Lambda^{-1}\left[A(x_\omega)x + B\right]. \tag{15}$$

By a lengthy computation (that we omit in this conference paper), it can be shown that if (13) holds, then $\dot{V}$ is a negative definite quadratic form in $\hat{x}$. From a classical stability result, see Theorem 4.10 (p. 154) in Khalil (2002), this system is globally exponentially stable. □

Note that the last proposition implies that x^e is the only equilibrium point of $\dot{x} = \tilde{G}(x)$, hence the TICSG system has exactly one equilibrium point in $\mathcal{E}$.

6. THE SYNCHRONIZATION RESULT

We prove that if the initial state of the TICSG model (5) is such that $|e(0)|$ is small enough, then, under some conditions, the state of the TICSG system will converge to the unique equilibrium point in $\mathcal{E}$. Thus, the region of attraction of this equilibrium point contains a neighborhood of positive thickness of any compact subset of $\mathcal{E}$.

Consider a system of the form

$$\dot{e} = F(e, x), \quad \dot{x} = G(e, x), \tag{16}$$

where e and x are real vector valued functions of dimensions n_e and n_x, respectively and $F, G \in C^2$ with $F(0, x) = 0$. Let $\mathcal{K}$ be an invariant compact subset of $\mathbb{R}^{n_e} \times \mathbb{R}^{n_x}$. We assume that the system is *forward complete on* $\mathcal{K}$, meaning that for every $(e_0, x_0) \in \mathcal{K}$, the solution $e(e_0, x_0, t), x(e_0, x_0, t)$ of (16) exists for all $t \geq 0$. We denote

$$\mathcal{K}_x = \{x \in \mathbb{R}^{n_x} \mid (0, x) \in \mathcal{K}\}.$$

Proposition 6.1. Suppose that the system (16) is such that $\dot{\tilde{x}} = G(0, \tilde{x})$ is globally exponentially stable on $\mathcal{K}_x$, with the equilibrium point $x^e \in \mathcal{K}_x$. Moreover, we assume that the matrix $\frac{\partial F}{\partial e}(0, x^e)$ is stable (Hurwitz). Then for every compact set K_x contained in the interior of $\mathcal{K}_x$ there exists $\varepsilon > 0$ such that the set

$$K(\varepsilon) = \left\{(e, x) \in \mathbb{R}^{n_e} \times \mathbb{R}^{N_x} \mid |e| \leq \varepsilon,\ x \in K_x\right\}$$

is contained in the region of attraction of the equilibrium point $(0, x^e)$ of (16).

Proof. It is easy to see that $(0, x^e)$ is an exponentially stable equilibrium point for the system (16) (because its linearization is Hurwitz). Let $\mathcal{N}$ be an open neighborhood of $(0, x^e)$ contained in its region of attraction. For each $x_0 \in K_x$ there exists $t > 0$ such that $x(0, x_0, t) \in \mathcal{N}$. Taking preimage through the flow, it follows that there exists an open neighborhood $\mathcal{M}(x_0)$ of $(0, x_0)$ contained in the region of attraction of $(0, x^e)$. We can find an open neighborhood $\tilde{\mathcal{M}}(x_0)$ of x_0 and a number $\varepsilon(x_0) > 0$ such that

$$\{e \in \mathbb{R}^{n_e} \mid |e| < \varepsilon(x_0)\} \times \tilde{\mathcal{M}}(x_0) \subset \mathcal{M}(x_0).$$

All the sets $\tilde{\mathcal{M}}(x_0)$ (for all $x_0 \in K_x$) are an open covering of the compact set K_x. We extract a finite covering $\tilde{\mathcal{M}}(\xi_1), \ldots \tilde{\mathcal{M}}(\xi_n)$ of K_x, and we take

$$\varepsilon = \min\{\varepsilon(\xi_j) \mid j \in \{1, \ldots n\},$$

then clearly the statement in the proposition holds. □

Now we return to our TICSG model, where F is as in (11) and G is as in (12). The linearization of F with respect to e has the same structure of the linearization of a system of a single generator connected to an infinite bus around it equilibrium point (as computed in Natarajan et al. (2015), formula (3.4)):

$$\frac{\partial F(e,x)}{\partial e}(0,x) = \begin{bmatrix} -\frac{R_s}{L_s} & \frac{x_\omega}{2} & \frac{x_q}{2} & -\frac{R_L}{L_s}x_q \\ -\frac{x_\omega}{2} & -\frac{R_s}{L_s} & -\frac{x_d}{2} - \frac{mi_f}{L_s} & \frac{R_L}{L_s}x_d \\ 0 & \frac{mi_f}{J} & -\frac{D_p}{J} & 0 \\ 0 & 0 & 1 & 0 \end{bmatrix}.$$

It follows from Proposition 5.1 that if (13) holds and moreover the above matrix (computed at the equilibrium point) is stable, then the conditions of Proposition 6.1 hold, so that its conclusion holds for the TICSG system.

It is possible to bring the TICSG system very close to the manifold $\mathcal{E}_\mathcal{X}$ by applying something called virtual friction, as discussed in Brown et al. (2014). There is no space here to explain the details.

7. SIMULATIONS

Our first simulation example concerns a TICSG system with two 5KW SGs where the parameters satisfy the conditions at the end of Section 6. The second example is such that the generators parameters again satisfy the conditions, but the manifold $\mathcal{E}_\mathcal{X}$ is only locally stable. Most parameters are the same as in the first simulation, but L_s is much smaller here. For this example we show a simulation that start inside the region of attraction and therefore the two generators synchronise, and another simulation with the initial state outside the region of attraction.

In each simulation result, the behavior of i_d and i_q over time is described for both SGs. We also plot the frequency ω and the phase difference between the two SGs δ as functions of the time. In all simulations, the value of T_m is chosen such that the equilibrium frequency is $\omega^e = 2\pi \cdot 50$.

The the simulation for the first example, shown in Figure 3, the TICSG system starts form the initial condition $[z_1(0)\ z_2(0)\ \delta(0)]^\top = [-400,\ -200,\ 10,\ 700,\ -20,\ 400,\ 1.5708]^\top$. The system synchronizes and converges to the equilibrium point $[z^e\ z^e\ \delta^e]^\top$. The parameters for this simulation are $J = 0.2\ [kg \cdot m^2]$, $D_p = 1.7\ [J \cdot sec]$, $R_s = 0.152\ [\Omega]$, $R_L = 18.862\ [\Omega]$, $L_s = 4.4\ [mH]$, $mi_f = 1.05\ [V \cdot sec]$, $T_m = 543.2031\ [N \cdot m]$.

Our further simulations of this system suggest that this TICSG system is globally asymptotically stable (GAS).

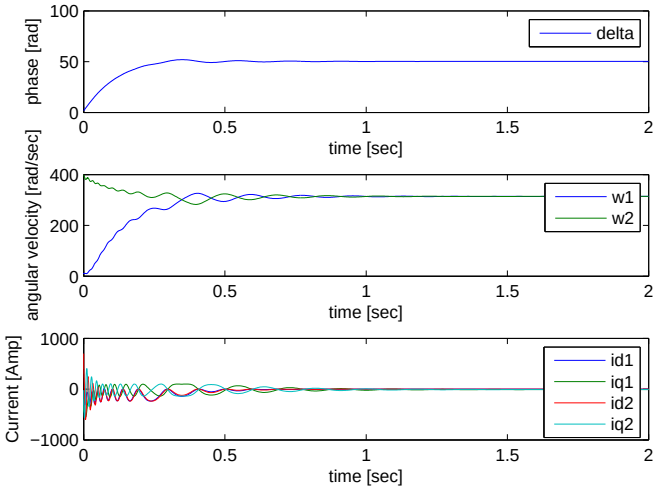

Fig. 3. Simulations for TICSG system with 5KW SGs

Figure 4 shows a simulation of a TICSG system similar to the previous one, but with smaller L_s, namely $L_s = 0.41\ [mH]$ (the other parameters are the same). The initial state is close to $\mathcal{E}$, $[z_1(0)\ z_2(0)\ \delta(0)]^\top =$

$[40,\ -20,\ 70,\ 400,\ -20,\ 65,\ 0]^\top$, such that the system stabilizes (in particular, the SGs synchronize).

Figure 5 shows another simulation for the same system, with the initial state $[z_1(0)\ z_2(0)\ \delta(0)]^\top = [-400,\ -200,\ 10,\ 700,\ -20,\ 400,\ 1.5708]^\top$. The simulation indicates that this initial state is outside the region of attraction, the SGs do not synchronize.

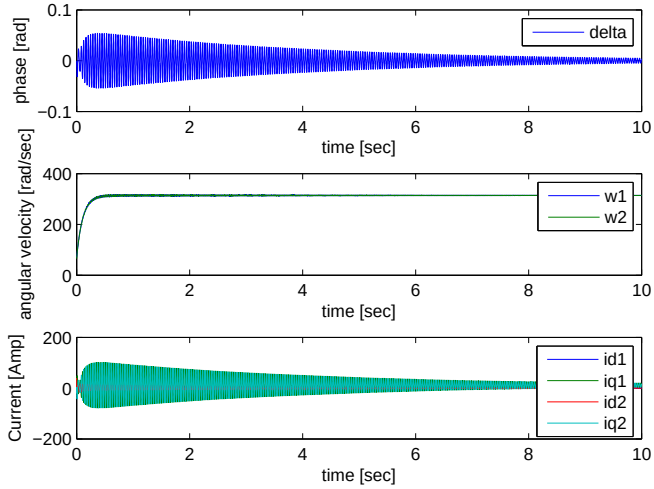

Fig. 4. Simulation for a TICSG system that satisfies the conditions at the end of Section 6, with initial state inside the region of attraction of the stable equilibrium point.

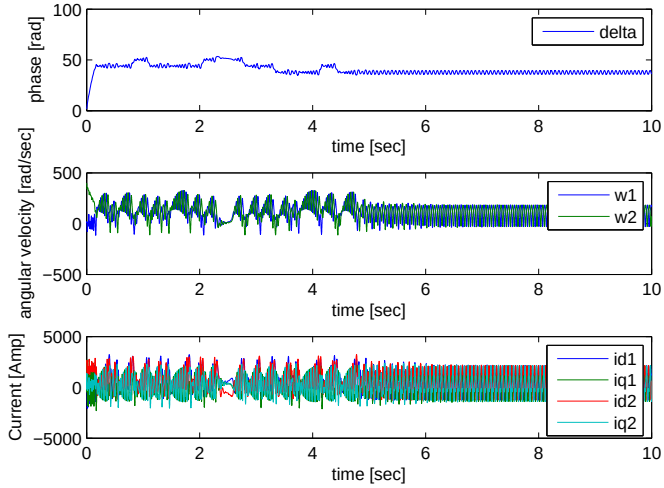

Fig. 5. Simulation for a TICSG system which satisfy the conditions at the end of Section 6, with initial state outside the region of attraction of the stable equilibrium point.

REFERENCES

E. Brown, and G. Weiss, Using synchronverters for power grid stabilization, *IEEE Convention of Electrical and Electronics Engineers in Israel*, Eilat, Dec. 2014.

S.Y. Caliskan, and P. Tabuada, Compositional transient stability analysis of multimachine power networks, *IEEE Trans. Control of Network Syst.*, vol. 1, 2014, pp. 4-14.

F. Dörfler, and F. Bullo, Synchronization and transient stability in power networks and nonuniform Kuramoto oscillators, *SIAM J. Control and Optim.*, vol. 50, 2012, pp. 1616-1642.

A.E. Fitzgerald, C. Kingsley, and S.D. Umans, *Electric Machinery*, McGraw-Hill, New York, 2003.

M. Galaz, R. Ortega, A.S. Bazanella, and A.M. Stankovic, An energy-shaping approach to the design of excitation control of synchronous generators, *Automatica*, vol. 39, 2003, pp. 111-119.

J.J. Grainger, and W.D. Stevenson, *Power Systems Analysis*, McGraw-Hill, New York, 1994.

T. Green, and M. Prodanovic, Control of inverter-based micro-grids, *Electric Power Systems Research*, vol. 77, 2007, pp. 1204-1213.

H.K. Khalil, *Nonlinear Systems* (third edition), Prentice Hall, New Jersey, 2002.

P. Kundur, *Power System Stability and Control*, McGraw-Hill, New York, 1994.

Y. Mandel and G. Weiss, Adaptive internal model based suppression of torque ripple in brushless DC motor drives, *Systems Science & Control Engineering*, vol. 5, 2015, pp. 162-176.

P. Monshizadeh, C. De Persis, N. Monshizadeh, and A. van der Schaft, Nonlinear Analysis of an improved swing equation, subm. 2016.

V. Natarajan, and G. Weiss, Almost global asymptotic stability of a constant field current synchronous machine connected to an infinite bus, *Proc. of the 53rd IEEE Conf. on Decision and Control*, Los Angeles, CA, Dec. 2014, pp. 3272-3279.

V. Natarajan, and G. Weiss, Almost global asymptotic stability of a grid-connected synchronous generator, submitted in 2015.

P. W. Sauer, and M. A. Pai, *Power Systems Dynamics and Stability*, Stipes Publishing, Champaign, IL, 1997.

Q. Shafiee, V. Nasirian, J.C. Vasquez, J.M. Guerrero, and A. Davoudi. A multi-functional fully distributed control framework for AC microgrids, *IEEE Trans. on Smart Grid*, to appear in 2016.

J. Schiffer, D. Zonetti, R. Ortega, A. Stanković, T. Sezi, and J. Raisch, A survey on modeling of microgrids - from fundamental physics to phasors and voltage sources, *Automatica*, vol. 74, 2016, pp. 135-150.

J.W. Simpson-Porco, F. Dörfler, and F. Bullo, Synchronization and power sharing for droop-controlled inverters in islanded microgrids, *Automatica*, vol. 49, 2013, pp. 2603-2611.

E. Venezian, and G. Weiss, A warning about the use of reduced models of synchronous generators, *Int. Conf. on the Science of Electrical Engineering* (ICSEE), Eilat, November 2016.

J.H. Walker, *Large Synchronous Machines: Design, Manufacture and Operation*, Oxford University Press, Oxford, 1981.

Q.-C. Zhong, Robust droop controller for accurate proportional load sharing among inverters operated in parallel, *IEEE Trans. on Industrial Electronics*, vol. 60, 2013, pp. 1281-1290.

Q.-C. Zhong, and G. Weiss, Synchronverters: Inverters that mimic synchronous generators, *IEEE Trans. Industr. Electronics*, vol. 58, 2011, pp. 1259-1267.